

Estimation of surface properties for art paintings using a six-band scanner

Shoji Tominaga, Suguru Nakamoto, Keita Hirai and Takahiko Horiuchi

Graduate School of Advanced Integration Science, Chiba University, Japan

Email: shoji@faculty.chiba-u.jp

The imaging systems using cameras to archive art paintings have several essential problems including image resolution and lens distortion. A scanner is considered as a precise imaging device, which can acquire images with high resolution and without camera lens distortion. The present paper proposes a method to estimate the surface properties of art paintings for digital archiving using the six-band scanner as a multiband spectral imaging system. The surface properties include surface-spectral reflectance and surface shape. The performance of the proposed method is compared with the previous studies that used the multiband imaging method by digital cameras. The current method has not only found to be as precise as the multiband imaging method in estimation accuracy, but also accompanied with several additional advantages.

Received 31 October 2013; revised 21 May 2014; accepted 21 May 2014

Published online: 15 July 2014

Introduction

The traditional techniques of image capture used to archive artworks in most museums of the world relied on conventional photographic processes. In 1989, the European Union founded a project to develop the first digital archiving system based on a CCD camera and six independent colour channels [1]. The system, called the VASARI, moved the digital camera to multiple positions across the painting area, and the images taken at each position were combined to create full high-resolution six-band image data. Miyake *et al.* developed a multiband camera system to record the reflectance spectra of art paintings [2]. The system consisted of a single-chip CCD camera and a rotating filter wheel comprised of five colour filters. CRISATEL was a European Union project begun in 2001 in the field of conservation and restoration of canvas paintings. The project developed a multispectral imaging system that was composed of a high-resolution CCD camera equipped with 13 narrowband interference filters, and of an electronically controlled lighting system [3]. Tominaga *et al.* proposed a technique for viewpoint- and illumination-independent digital archiving of paintings [4]. They acquired images of a painting using a multiband imaging system with six spectral channels. All those works used camera systems for acquiring surface properties of paintings. However, camera systems have the following essential problems: (1) resolution is not enough, (2) there is a lens distortion, (3) imaging system is complicated, and (4) the cost is expensive.

A scanner is considered as a precise imaging device for document and objects with flat surface. The device can acquire images with high resolution and without camera lens distortion. However, traditional three colour scanners could suffer from colour reproduction errors due to the significant mismatch between their spectral sensitivities and those of the human visual systems. Recently, a scanner was developed for capturing additional colour channels to reduce the colour reproduction errors [5]. The novel scanner captures six colour channels in total from two separate scans using two different fluorescent lamps. Previously we investigated fundamental properties of the six-band scanner and showed the usefulness for estimating the spectral reflectance function of an object surface [6].

This paper proposed a method to estimate the surface properties of art paintings for digital archiving using the six-band scanner as a multiband spectral imaging system. The surface properties include the reflectance information of surface-spectral reflectance and the shape information of surface normal and height. We aim at recovering such surface physical properties from the scanner image data.

A painting's surface on the scanning plane is illuminated by light sources with two different spectral properties from two directions. Then use of two sets of RGB sensor outputs for two scans constitutes a six-band scanner system. Moreover, Image acquisition of the same surface is repeated in different scanning directions for the purpose of reliable estimation of the surface properties. We present estimation algorithms based on six-dimensional image data without specular reflection and shadow. The performance of the proposed method is examined in experiments in detail, compared with the previous multiband imaging methods.

Imaging system

Multiband scanner

Figure 1 draws a schematic diagram of the six-colour scanner. An object on the scanning plane is illuminated by light bulbs L1 and L2 with two different spectral properties from two directions. The scanner system uses a single three colour CCD and two different cold cathode fluorescent lamps for two scans. The phosphor selection of the lamps is described in Ref. [5] in detail. We measured the spectral power distributions of two scanner lamps. In Figure 2 (Left), the solid curve (Bulb1) shows the spectral distribution of a standard white lamp. The dashed curve (Bulb2) shows the different spectral distribution of the second blue lamp. The spectral intensity of this lamp is higher in shorter wavelength of the visible range than one in longer wavelengths. Figure 2 (Right) shows the overall scanner spectral response functions by combing the spectral power distributions of the lamps and the spectral sensitivities of RGB sensors. The solid curves (Bulb1) represent the red, green, and blue responses for the standard white lamp, and the dashed curves (Bulb2) represent the red, green, and blue responses for the second blue lamp.

The scanner outputs are quantised in 16 bits and normalised with a white reference at every scan. We investigated the linearity of the responses for reflecting objects. The Munsell Neutral Value Scale with 37-step scale was used as a set of grey scale samples. We confirmed that a good linear relationship is obtained in both scans.

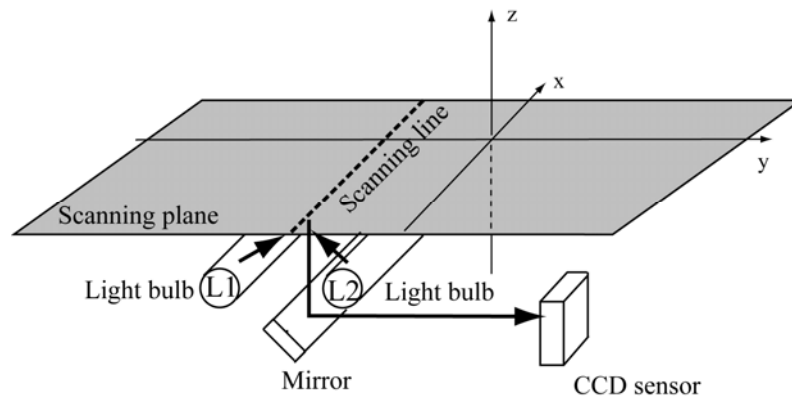


Figure 1: Schematic diagram of the scanner used in this study.

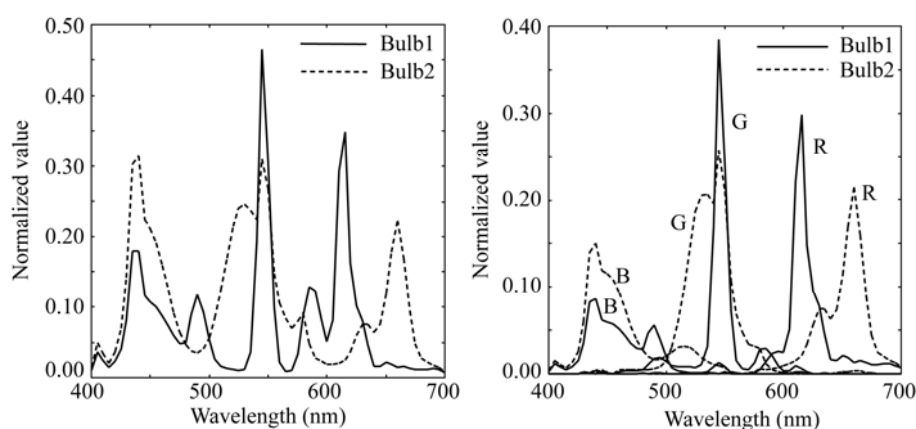


Figure 2: Spectral responses of the six-band scanner. Spectral power distributions of scanner lamps (left). Overall scanner spectral response functions (right).

Surface observation

The normalised RGB sensor outputs for the two scans are modelled as a linear system

$$\begin{bmatrix} r_i \\ g_i \\ b_i \end{bmatrix} = \int_{400}^{700} S(\lambda) E_i(\lambda) \begin{bmatrix} R(\lambda) \\ G(\lambda) \\ B(\lambda) \end{bmatrix} d\lambda, \quad (i=1, 2) \quad (1)$$

where $S(\lambda)$ is the spectral reflectance of a painting's surface, $E_i(\lambda)$ ($i=1, 2$) are the spectral power distributions of the white and blue light sources shown in Figure 2 (Left), and $(R(\lambda), G(\lambda), B(\lambda))$ are the spectral sensitivity functions of RGB sensors. When we take any noisy observations into account, two sets of sensor outputs are summarised as a six-dimensional linear system

$$\rho_i = \int_{400}^{700} S(\lambda) H_i(\lambda) d\lambda + n_i, \quad (i=1, 2, \dots, 6) \quad (2)$$

where the spectral response functions $H_i(\lambda)$, shown in Figure 2 (Right), are defined as

$$\begin{aligned} H_1(\lambda) &= E_1(\lambda)R(\lambda), & H_2(\lambda) &= E_2(\lambda)R(\lambda), & H_3(\lambda) &= E_1(\lambda)G(\lambda), \\ H_4(\lambda) &= E_2(\lambda)G(\lambda), & H_5(\lambda) &= E_1(\lambda)B(\lambda), & H_6(\lambda) &= E_2(\lambda)B(\lambda) \end{aligned} \quad (3)$$

and n_i are the noise component with zero mean, including image sensor noise and an approximation error in the model.

The painting's surface is regarded as a 3D rough surface including specular reflection and shadow. For the purpose of reliable estimation of surface-spectral reflectance and surface normal, the image acquisition of the same surface is repeated for different illumination directions. The position of the sensor is fixed. To perform different illumination directions to the painting's surface, we observe the same painting at eight scanning directions as shown in Figure 3. The algorithm of Scale-Invariant Feature Transform (SIFT) is used for alignment of images observed in different directions [7]. It enables accurate alignment by extracting local features of the respective observed images and using an affine transformation.

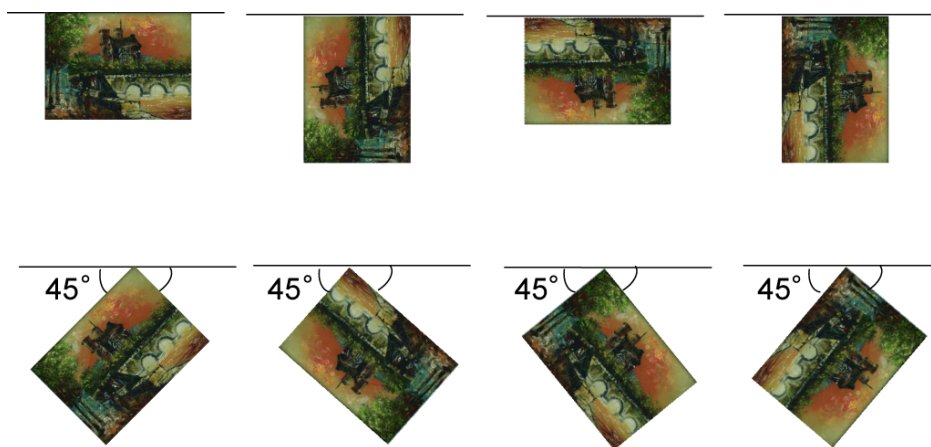


Figure 3: Observations of the same painting at different scanning directions.

Estimation algorithms of surface properties

Data selection

A painting's surface is not always flat in pixel points and has often difference in height level. Since the sensor outputs are based on light reflected from the surface. The outputs by the two scanning ways vary according to the surface shape. Figure 4 illustrates the effect of shading for a painting's surface with difference in height level. The slanting rays of either light source casts the shadow of the higher surface onto the lower surface. The sensor outputs for the shadow area decrease much, compared with ones in any other surface area, because the surface is shielded by another surface from the light source.

In such an area, the six sensor outputs by the two scans are too unreliable to estimate the surface-spectral reflectance function and the surface normal. When examining that each point of the surface is properly illuminated by a light source, we notice that the shadows occurs only once in the two scans. If the pixel point belongs to the shadow area, we discard the RGB outputs of the corresponding scan and use the remaining RGB outputs of the other scan for the surface estimation. Examination of shading can be performed easily by intensity comparison between two RGB vectors by the two scans as follows:

$$\sqrt{r_1^2 + g_1^2 + b_1^2} / \sqrt{r_2^2 + g_2^2 + b_2^2} \geq T \quad (4)$$

where T is a certain threshold. If a pixel point satisfies the above condition, we take only the sensor outputs (r_1, g_1, b_1) under the light source 1 for the estimation.

Next, let us consider a glossy surface like oil painting. The surface material of an oil painting consists of a thick oil layer. It is sometimes coated with varnish to protect the painting's surface and to bring out the colours, so a strong gloss, or highlights, appears on the surface. A criterion function similar to Eq. (4) is available for detection of the highlight area by specular reflection. If a pixel point belongs a highlight area, satisfies the above inequality, we take only the sensor outputs (r_2, g_2, b_2) under the light source 2 for the estimation.

Surface-spectral reflectance and surface normal are estimated using scanner data belonging to the diffuse component at each pixel point of the multiple images acquired under different scanning directions. If the sensor output is judged to be based on a highlight or a shadow, the observation is neglected from the data set for both estimations.

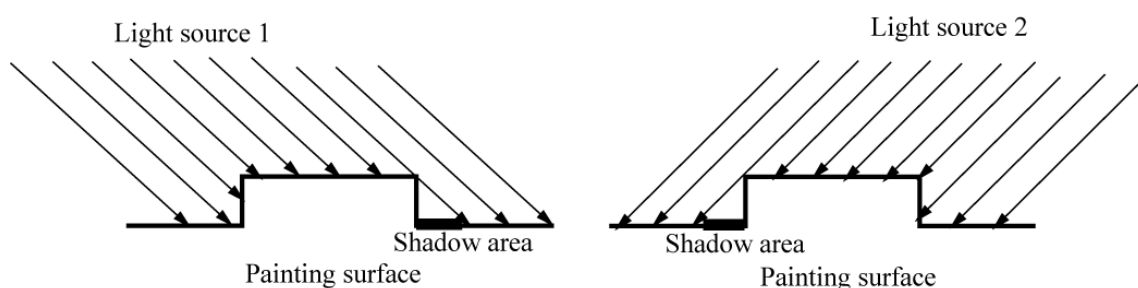


Figure 4: Shading effect for a painting's surface with difference in height level.

Spectral reflectance estimation

The standard white matte paper is used for correcting the local non-uniformity of illumination and normalising all spectral reflectances to the vertically incoming ray. The sensor outputs are then normalised in the form, ρ_{ij}/ρ_{wij} , where ρ_{ij} denotes the output of i -th sensor under j -th scanning direction and ρ_{wij} is the i -th sensor output for the standard white paper under the j -th direction. These normalised sensor outputs are finally averaged on directions, j .

We assume that each spectral function in Eq. (2) is sampled at 61 points with an equal interval $\Delta\lambda$ (5 nm) in the region [400nm, 700nm]. Let \mathbf{S} be a 61-dimensional column vector representing the spectral reflectance $S(\lambda)$, \mathbf{H} be a 6×61 matrix with the element $h_{ij} = E(\lambda_j)R_i(\lambda_j)\Delta\lambda$, $\boldsymbol{\rho}$ be a 6D column vector representing the sensor outputs, and \mathbf{n} be a 6D noise column vector. Then Eq. (2) is described in a matrix equation.

$$\boldsymbol{\rho} = \mathbf{H}\mathbf{s} + \mathbf{n} \quad (5)$$

When the signal component \mathbf{S} and the noise component \mathbf{n} are uncorrelated, an optimal linear estimator to minimise the mean-squared error is given by the Wiener estimator (see [4]):

$$\mathbf{S} = \mathbf{C}_{SS} [\mathbf{H}\mathbf{C}_{SS}\mathbf{H}^T + \sigma^2\mathbf{I}]^{-1} \boldsymbol{\rho}. \quad (6)$$

where σ^2 is the noise variance, \mathbf{I} is a 61×61 unit matrix, and \mathbf{C}_{SS} is a 61×61 correlation matrix that is statistically determined as $\mathbf{C}_{SS} = \mathbf{E}[\mathbf{ss}^T]$. The symbol T denotes a matrix transpose. To determine \mathbf{C}_{SS} , we used a database of measured surface spectral reflectances of many sample surfaces applied with different paints.

Estimation of surface normal

A photometric stereo method [8] is used to estimate the surface normal vector at each pixel point of an observed painting's surface. If the painting's surface is a perfect diffuser (Lambertian), the surface normal vector can numerically be estimated using images acquired at three different illumination directions, that is, three different scanning directions.

The estimates of surface orientation should not depend on the surface colours. Therefore, we fit the scanner spectral response functions to the CIE standard luminosity function $V(\lambda)$ of the human visual system as

$$V(\lambda) = \sum_{i=1}^6 c_i H_i(\lambda). \quad (7)$$

Then, the scanner outputs at a pixel (x, y) are converted into the approximated luminance value as

$$I(x, y) = w \sum_{i=1}^6 c_i \rho_i, \quad (8)$$

where w is a scaling factor.

Since the painting's surface is observed at the eight illumination directions by rotating the paintings on the scanning plane, let $\mathbf{I} = [I_1, I_2, \dots, I_8]$ be a 1×8 matrix of the observed luminance values at a pixel point. The assumption of diffuse reflection gives us the relationship

$$\mathbf{I} = \alpha \mathbf{N}^T \mathbf{L}, \quad (9)$$

where \mathbf{N} is a surface normal vector and \mathbf{L} is a 3×8 matrix showing a set of illumination directional vectors. Therefore an estimate $\hat{\mathbf{N}}$ of the surface normal is obtained as the least squared solution $\hat{\mathbf{N}} = \mathbf{L}^+ \mathbf{I}^T / \alpha$, where \mathbf{L}^+ is a generalised inverse of \mathbf{L} . In the present scanner, the incident angle of the light source relative to a flat surface was determined to be 45 degrees. Therefore, the illumination directional matrix \mathbf{L} is then given by

$$\mathbf{L} = \begin{bmatrix} 1/\sqrt{2} & 0 & -1/\sqrt{2} & 0 & 1/2 & -1/2 & 1/2 & -1/2 \\ 0 & 1/\sqrt{2} & 0 & -1/\sqrt{2} & 1/2 & 1/2 & -1/2 & -1/2 \\ 1/\sqrt{2} & 1/\sqrt{2} \end{bmatrix}. \quad (10)$$

Estimation of surface height

In principle, height information of an object surface can be reconstructed from the surface normal vectors by using the consistent gradient operator [9, 10]. However, the painting's heights inevitably suffer from low-frequency distortion, because of the surface-normal vectors estimated from the noisy and uneven surface of canvas fabric or panel. To improve estimation accuracy of the surface height, we incorporate a small number of direct measurements of surface height by using a laser scanning meter. The meter used in this paper is a Keyence laser confocal displacement meter. A painting surface is scanned with high accuracy and resolution of 0.2 μm . Note that, although accurate surface height is measured directly, it takes too much time to measure even a small painting in high resolution. Therefore, it is only available for measuring accurate surface heights at a small number of locations. In our experiments, twenty-one locations are taken to be able to cover uneven surface.

A computational procedure is shown for accurate surface reconstruction by combining the direct height measurements and the estimated surface normal vectors [11]. First, to determine a smooth surface, these measurement points are interpolated using a 3rd order spline function. A fast Fourier

transform (FFT) of the smooth surface provides low-frequency components of the surface basis. On the other hand, we estimate surface height from the surface normals by using the Chellappa-like algorithm with the integrability and distortion reduction. This FFT provides reliable estimates of the surface height for the higher frequency part. Therefore, we discard the low-frequency part of this high-resolution height estimates, and substitute the low-frequency components of the direct measurements for the corresponding frequency part of the high-resolution estimates. The precise shape of a painting surface is reconstructed from an IFFT of the whole composite frequency components.

Experiments

Multiband camera system

For the purpose of performance comparison in surface property estimation, we used two imaging systems based on digital cameras and a projector. These systems were used for estimating surface properties of various paintings in our previous studies [12]. One is a multiband imaging system, and another is a high-resolution imaging system.

The multiband imaging system is used for estimating the surface-spectral reflectance function. This system is decomposed into a monochrome camera and a multispectral lighting system. The camera is a Toshiba Teli camera with a 1636×1236 pixel size and a 10 bit quantisation. The lighting system consists of a slide projector and six colour filters. The combined system provides a stable imaging system with six spectral bands in the wavelength range of 400 to 700 nm. The spectral reflectance of a painting's surface is recovered by applying the Wiener estimator to the six band camera outputs in the same manner as Eq.(6).

The high-resolution imaging system is used for precisely estimating the surface normals of small facets on a painting's surface. The camera is a Canon EOS camera with a 5634×3753 pixel size, RGB channels, and a 14-bit quantisation level. The lighting system uses the same projector of a white light source without colour filters. The surface normal vectors are estimated using the photometric stereo method. The painting surface is observed at the nine illumination directions, which composite four directions at 60 degrees and 45 degrees angle of incidence for the painting, respectively, and one direction from the top of the painting. Because we use the luminance value for normal estimation at each pixel, we fit the RGB spectral sensitivities, $R(\lambda)$, $G(\lambda)$, and $B(\lambda)$, to the luminosity function $V(\lambda)$ and convert the camera outputs (r, g, b) to the luminance value in the same way as Eq.(8).

Image resolution

For investigating the resolution of images acquired by the present scanner system, we used the freeware (Olympus HYRes 3.1) of accurately gauging the resolution of a digital camera in which a resolution chart shown in Figure 5 was used on the basis of ISO 12233 standard. In this chart, we used the red and blue patterns. As a result, we had limit resolutions of 4905 LW/PH and 2721 LW/PH for the scanner and the high-resolution camera, respectively. The unit LW/PH means the Line Width per Picture Height, where PH=200mm in this paper. The number of 4905 represents about 25 lines per one millimetre. That is, 25 lines per one millimetre can be solved. We confirmed that the image resolution was improved by using the present scanner system.

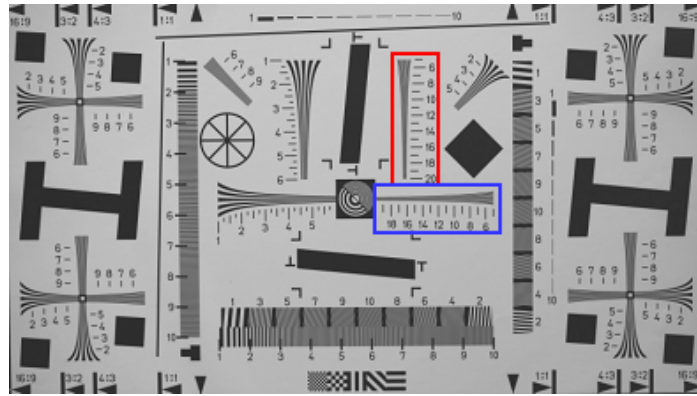


Figure 5: ISO standard chart used for resolution evaluation.

Distortion

A checkerboard pattern of 23×17 shown in Figure 6 (Left) was used to investigate the property of lens distortion in the camera system. We checked the corner points in the pattern on the captured image. The size of captured image was 3606×4944 . Figure 6 (Right) shows a 3D graph of the amount of shift of each corner point on the captured image. The lowest peak point corresponds to the lens center. The distortion increases as the position is distant from the lens center. The average and maximum distortions were 10.85 and 16.11 pixels, respectively. On the other hand, there was no distortion at all points in the scanner system. We confirmed that the camera lens distortion was completely removed in using the scanner system.

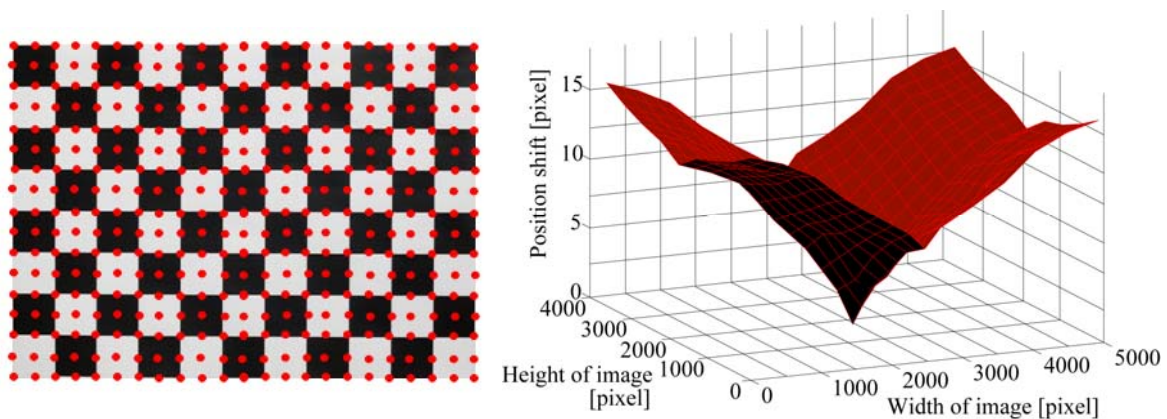


Figure 6: Lens distortion in the camera system. Checkerboard pattern of 23×17 (left). 3D graph of the amount of shift of each corner point on the captured image (right).

Spectral reflectance

Figure 7 shows an oil painting called “River” in our collection of art paintings. The estimation accuracy was examined at 20 points on the painting’s surface shown in Figure 7. Figure 8 shows the estimated spectral reflectances at the 20 points by using the proposed scanner system and estimation algorithm. The red curve in each figure represents the estimate, and the black curve represents the direct measurement by a spectro-radiometer. The root mean square error (RMSE) was calculated between the estimation and the measurement. The averaged error in 20 points was 0.0275. On the other hand, the reflectance estimation was performed based on the multiband image data captured by the above six-band camera system. The averaged error for the camera system was 0.0284. The six-

band scanner system performs the spectral estimation accuracy as precise as the six-band camera system.



Figure 7: Oil painting "River".

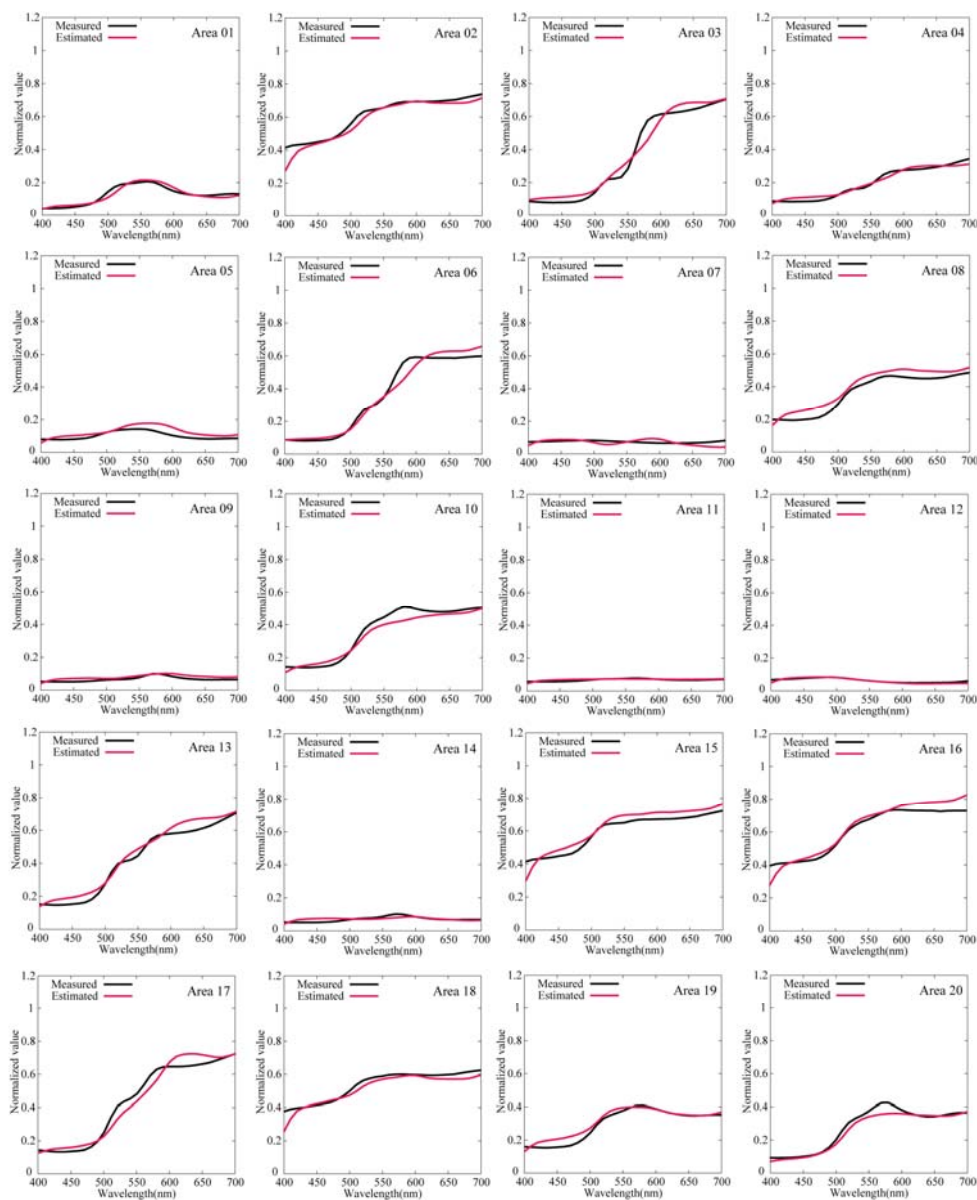


Figure 8: Estimated spectral reflectances at the 20 points by using the proposed system and algorithm.

Surface normal

Figure 9 shows the estimation results of surface normal vectors at all pixel points. The directional vectors are rendered using a colour map. The vertical direction corresponds to white. The upper left picture in Figure 9 shows the estimated surface normal vectors from the image data by the scanner system, and the upper right picture shows the estimation results from the image data by the high-resolution camera data. The lower picture shows the direct measurements by a laser displacement meter. The averaged errors of the estimated surface normal vectors were 9.77° and 9.25° for the scanner and the camera, respectively.

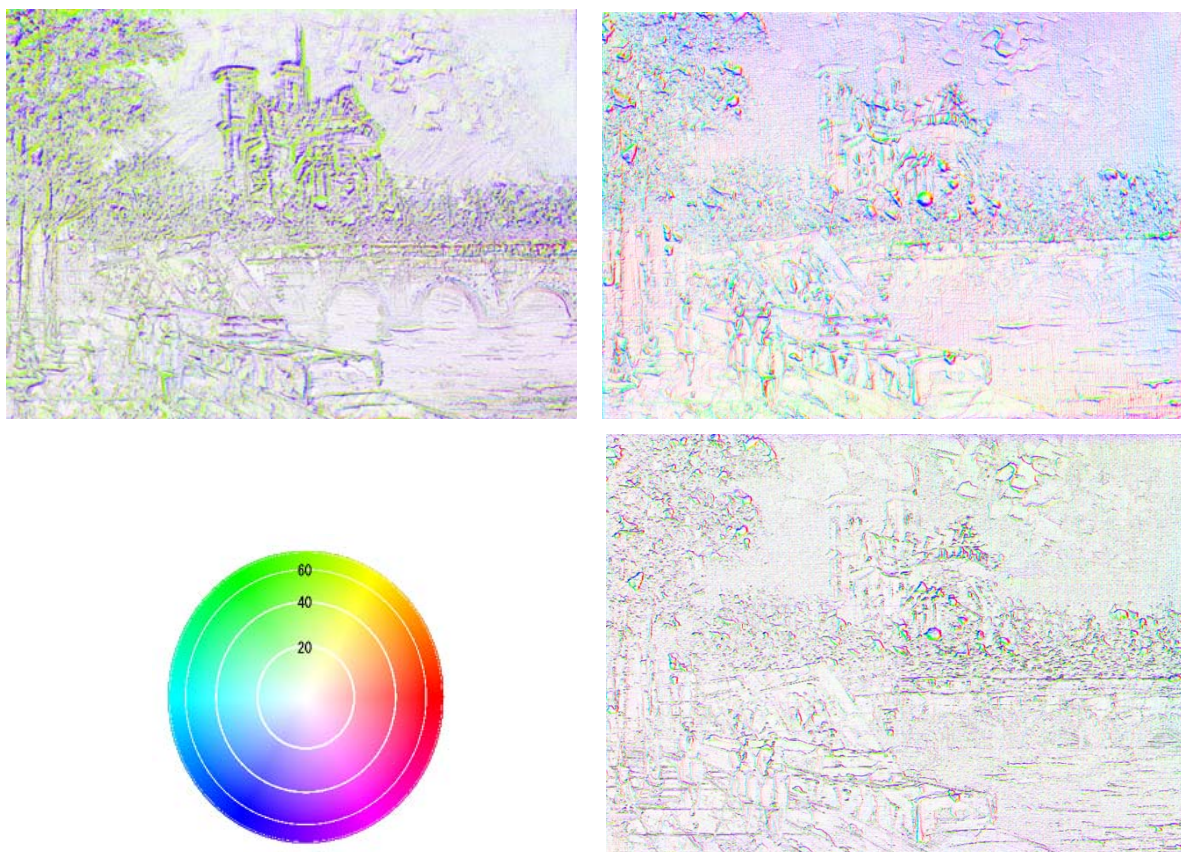


Figure 9: Estimated surface normal vectors. Estimation results from image data by the scanner system (upper left). Estimation results from image data by the high-resolution camera data (upper right). Colour map of directional vectors (lower left). Direct measurements by a laser displacement meter (lower right).

Surface height

Figure 10 shows the surface reconstruction results. Figure 10 (left) depicts the estimated surface shape of the painting's surface based on the image data by the scanner, which was obtained from the estimated surface-normal vectors in Figure 9 (upper left) and additionally from the measured heights at 12 locations by the confocal displacement meter. In the figure, the red mesh and the black mesh represent the estimated surface shape and the directly measured surface shape, respectively. Figure 10 (right) depicts the estimated surface shape based on the image data by the camera, which was obtained from the estimated surface-normal vectors in Figure 9 (upper left) and additionally from the same 12 height measurements as the above measurements. The average differences between the estimated 3D surface shapes and the direct measurements were $14.3\ \mu\text{m}$ and $14.0\ \mu\text{m}$ for the scanner

and the camera, respectively. The proposed scanner-based method has the surface reconstruction accuracy as precise as the camera-based method.

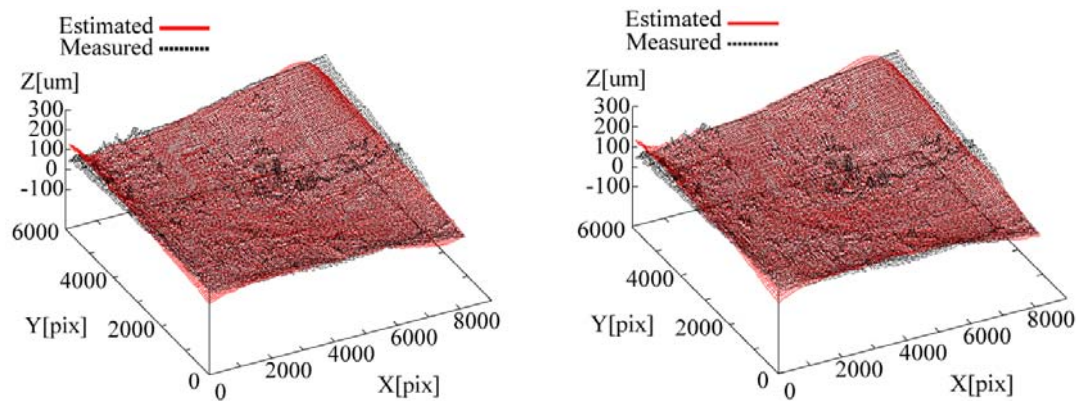


Figure 10: Surface reconstruction results for oil painting “River”. Estimated surface shape by the proposed scanner-based method (left). Estimated surface shape by the camera-based method (right).

Image rendering

Realistic images of the oil painting were rendered using the estimated surface-spectral reflectances and surface heights by the proposed scanner-based method. We used the Cook-Torrance model for describing light reflection of the oil painting’s surface. This model includes several parameters such as the index of refraction (n), the roughness index (m), and the specular coefficient (c_s/c_d). These parameters were determined as $m=0.06$, $(c_s/c_d)=76.9$, and $n=2.5$ for rendering the painting images. Figure 11 (left) shows the rendered image of “River”. We assumed that the surface was illuminated by an artificial sunlight lamp with the incident angle of 80 degrees from the upper direction. Figure 11 (right) shows a real photograph of the same painting taken under the same illumination conditions.

We compare the performance in the rendered images. Figure 12 (left) shows the close-up of a small part of the rendered image in Figure 11 (left). Figure 12 (right) shows the close-up of the same part of the rendered image, which is based on the estimated surface-spectral reflectances and surface heights by the camera-based method, where the illumination conditions are the same as the above image. We can easily understand that the left is fine resolution and the image is sharp. On the other hand, the right image is a little blurred.

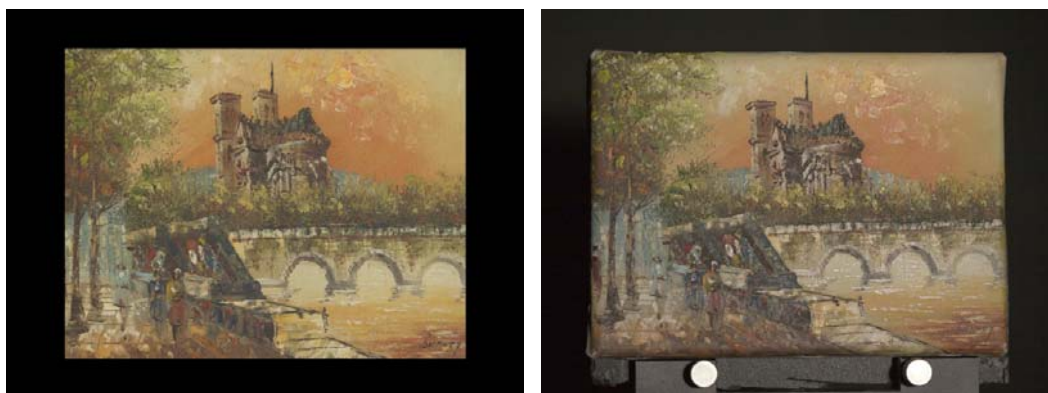


Figure 11: Image rendering result of the oil painting “River”. Rendered image based on the proposed scanner-based method (left). Real photograph of the same painting taken under the same illumination conditions (right).

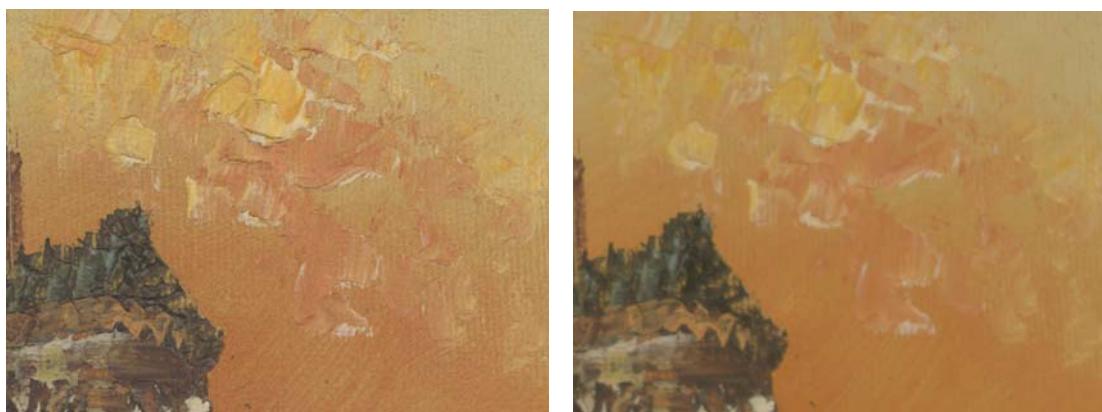


Figure 12: Close-up of the rendered images for the oil painting "River". (Left): Proposed scanner-based method. (Right): Camera-based method.

Performance comparison

Table 1 summarises the performance comparison between the proposed scanner-based system and the previous camera-based method. First, note that the image resolution of the present six-band scanner system is about twice of the high-resolution camera system. Second, the distortion error is zero for the scanner system, but the camera system has 10 pixels in average. Third, the estimation accuracy of the surface properties is almost the same in using two imaging systems. The scanner-based method has advantages as a multiband imaging system for digital archiving of oil paintings.

		Scanner-based method	Camera-based method
Resolution (LW/PH)		4905	2721
Mean distortion (pixel)		0	10.85
Spectral reflectance error (RMSE)		2.750×10^{-2}	2.840×10^{-2}
Surface normal error ($^{\circ}$)	Ave	9.77	9.25
	Max	86.55	60.30
	Min	1.704×10^{-3}	3.198×10^{-3}
Height error (μm)	Ave	14.33	14.04
	Max	164.6	175.9

Table 1: Comparison of experimental results between the proposed scanner-based method and the previous camera-based method.

Conclusions

The present paper has proposed a method to estimate the surface properties of art paintings for digital archiving using the six-band scanner as a multiband spectral imaging system. The painting's surface properties included the reflectance information of surface-spectral reflectance and the shape information of surface normal and height. We aimed at recovering the surface physical properties from the scanner image data. A painting's surface on the scanning plane was illuminated by light sources with two different spectral properties from two directions. The six-band scanner system was

constructed using two sets of RGB sensor outputs for two scans. Moreover, the image acquisition of the same surface was repeated in different scanning directions for reliable estimation of the surface properties. We presented estimation algorithms based on six-dimensional image data without specular reflection and shadow. The performance of the proposed method was examined in experiments in detail, which was compared with the previous multiband imaging method based on digital cameras. The proposed method has not only found to be as precise as the multiband imaging method in estimation accuracy, but also accompany with four advantages of (1) high image resolution, (2) no lens distortion, (3) compact imaging system, and (4) lower cost.

References

1. Martinez K, Cupitt J and Saunders D (1993), High resolution colorimetric imaging of painting, *Proc. SPIE*, 1901, 25–36.
2. Miyake Y, Yokoyama Y, Tsumura N, Haneishi H, Miyata K and Hayashi, J (1999), Development of multiband color imaging systems for recording of art paintings, *Proc. SPIE*, 3648, 218–225.
3. Shumitt F, Aitken G, Alquie G, Brettel H, Chouikha MB, Colantoni P, Cotte P, Cupitt J, de Deyne C, Dupraz D, Lahanier C, Liang H, Pilay R, Ribes A and Saunders D (2005), CRISATEL, *Proc. 10th Congress of International Colour Association*, 463–467.
4. Tominaga S and Tanaka N (2008), Spectral image acquisition, analysis, and rendering for art paintings, *Journal of Electronic Imaging*, **17** (4), 043022-1-13.
5. Hunter A, DiCarlo J and Pollard S (2008), Six color scanning, *Proc. CGIV*, 570-574.
6. Tominaga S, Kohno S, Kakinuma H, Nohara F and Horiuchi T (2009), Spectral reflectance estimation using a six-color scanner, *Proc. IS&T/SPIE Symposium on Electronic Imaging*, **7241**, 72410W.
7. Lowe D (2004), Distinctive image features from scale-invariant keypoints, *International Journal of Computer Vision*, **60** (2), 91-110.
8. Woodham R (1980), Photometric method for determining surface orientation from multiple images, *Optical Engineering*, **19** (1), 139-144.
9. Frankot RT and Chellappa R (1988), A method for enforcing integrability in shape form shading algorithms, *IEEE Transactions on Pattern Analysis and Machine Intelligence*, **10** (4), 439-451.
10. Ando S (2000), Consistent gradient operator, *IEEE Transactions on Pattern Analysis and Machine Intelligence*, **22** (3), 252-265.
11. Tominaga R, Ujike H and Horiuchi T (2010), Surface reconstruction of oil paintings for digital archiving, *Proc. IEEE Southwest Symposium on Image Analysis and Interpretation*, 173-176.
12. Tanimoto T, Horiuchi T and Tominaga S (2013), Precise estimation of painting surfaces for digital archiving, *Proc. 4th IAPR Computational Color Imaging Workshop (CCIW2013)*, Lecture Notes in Computer Science, LNCS 7786, 171-183, Springer-Verlag.
13. Cook R and Torrance K (1981), A reflection model for computer graphics, *Proc. SIGGRAPH 81*, **15** (3), 307-316.